

PHYSICAL REVIEW B

CONDENSED MATTER AND MATERIALS PHYSICS

THIRD SERIES, VOLUME 61, NUMBER 24

15 JUNE 2000-II

RAPID COMMUNICATIONS

Rapid Communications are intended for the accelerated publication of important new results and are therefore given priority treatment both in the editorial office and in production. A Rapid Communication in Physical Review B may be no longer than four printed pages and must be accompanied by an abstract. Page proofs are sent to authors.

DX-behavior of Si in AlN

R. Zeisel,* M. W. Bayerl, S. T. B. Goennenwein, R. Dimitrov, O. Ambacher, M. S. Brandt, and M. Stutzmann
 Walter Schottky Institut, Technische Universität München, Am Coulombwall, D-85748 Garching, Germany
 (Received 22 March 2000)

In Si doped AlN, a large persistent photoconductivity is found for temperatures below 60 K after exposure to light with photon energies above 1.5 eV. Simultaneously, a persistent electron spin resonance signal is observed with an isotropic g factor of 1.9885 due to an effective mass donor state, while no spin resonance signal is detectable after cooling the sample in the dark. Both observations show that Si undergoes a DX -like metastability in this material. Based on the experimental findings, a detailed configuration diagram is proposed.

Among the group III nitrides, the $Al_xGa_{1-x}N$ alloys especially play an increasing role in semiconductor devices such as high frequency/high temperature field effect transistors, surface acoustic wave filters, optoelectronic devices for UV detection and light emitting diodes in the blue and UV range. For n -type doping—e.g., in modulation doped field effect transistor structures¹—Si is most commonly used as the donor. However, some basic aspects of the behavior of this impurity are not understood up to now. In GaN, Si is known to be an effective mass donor. In $Al_{0.6}Ga_{0.4}N$ high pressure experiments have shown that Si forms a localized deep state instead.² From previous work concerning Si in $Al_xGa_{1-x}N$ it is known³⁻⁵ that Si— from a certain Al content up—can lower its energy by a large lattice relaxation and the capture of a second electron, the so called DX formation

$$2d^0 \rightleftharpoons d^+ + DX^- + U. \quad (1)$$

Here d denotes a substitutional shallow impurity and DX the displaced deep state. The superscripts specify the charge states. U stands for the correlation energy. Since the DX formation reaction leads to a self-compensation of the Si donor, it is of great fundamental as well as practical interest to check whether a similar reaction occurs in $Al_xGa_{1-x}N$ alloys with high Al content. So far, for Al-rich $Al_xGa_{1-x}N$ only theoretical work about the Si lattice relaxation exists. However, the theoretical predictions are contradictory: While Park and Chadi⁶ and Boguslawski and Bernholc⁷ have pre-

dicted that the DX state is the stable configuration for Si in AlN, van de Walle⁸ has argued that Si always remains a shallow effective mass donor over the whole composition range. In the case of oxygen in $Al_xGa_{1-x}N$ alloys, high pressure experiments on GaN as well as measurements of spectrally resolved and persistent photoconductivity (PPC) in $Al_xGa_{1-x}N$ have shown that for Al contents $x \geq 0.35$ this dopant exhibits a DX -like behavior.^{9,10} As mentioned above, there are already some results which point towards a Si-related localized state in $Al_{0.6}Ga_{0.4}N$.² However, the PPC observed at ambient pressures in these samples is very small and no spectral photoionization threshold is presented. Since PPC is also reported in pure GaN and low Al containing $Al_xGa_{1-x}N$ alloys^{11,12} and can have a variety of origins other than DX -like defects, EPR experiments will be essential to prove the DX nature of the defects responsible for PPC in $Al_xGa_{1-x}N$. Furthermore, the authors did not specify the Al concentration to which the applied pressure corresponds. Here, based on spectrally resolved photoconductivity and electron paramagnetic resonance (EPR) measurements, we show that Si indeed exhibits a DX -like relaxation in AlN.

The AlN:Si samples investigated here are 1.5 μm thick and were grown on (0001)-oriented sapphire substrates by plasma induced molecular beam epitaxy. The nominal Si doping density is $3 \times 10^{19} \text{ cm}^{-3}$. This high Si concentration ensures that the Fermi level is shifted from the position determined by the background oxygen impurity concentration

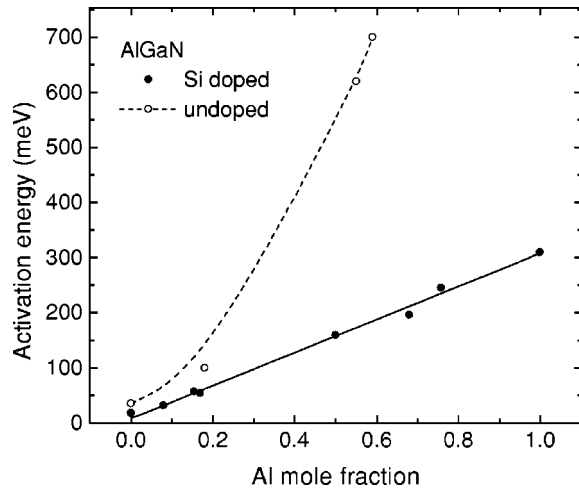


FIG. 1. Activation energies of Si-doped (full circles) and nominally undoped (open circles) $\text{Al}_x\text{Ga}_{1-x}\text{N}$. The lines are a guide to the eye.

of $1 \times 10^{18} \text{ cm}^{-3}$, as measured by elastic recoil detection analysis, to 320 meV below the conduction band. Hall effect measurements reveal a free electron concentration of $2 \times 10^{15} \text{ cm}^{-3}$ at room temperature. Photoconductivity experiments have been carried out at 20 K at an electric field of 200 V/cm using a halogen lamp in conjunction with a grating monochromator and appropriate filters to cut off higher orders. EPR experiments have been performed using a standard X-band EPR spectrometer with a TE_{102} microwave cavity. For g factor calibration, DPPH was used.

In Fig. 1 we show the activation energy of the dark conductivity for Si-doped $\text{Al}_x\text{Ga}_{1-x}\text{N}$ alloys over the whole composition range ($x=0 \dots 1$) (full circles). The activation energy increases linearly from 18 meV (GaN) to 320 meV (AlN). In contrast, the activation energy of similarly prepared but nominally undoped alloys are much higher (open circles). The role of oxygen and nitrogen vacancies as the usual residual donor in group-III nitrides therefore is negligible in our Si-doped MBE-grown samples.

Assuming a normal shallow donor character for Si in AlN, we would expect infrared absorption and photoconductivity at photon energies around 320 meV. However, such a behavior was not observed. Instead, as shown in Fig. 2 after cooling the sample to 20 K in the dark, there is a strong photoconductivity threshold at about 1.5 eV. This photocurrent, once excited, persists after switching off the light at as much as eight orders of magnitude above the dark current. The full symbols in Fig. 2 represent the spectrally resolved photoconductivity after cooling down the sample in the dark. The full line is the spectrum recorded after the first one without heating the sample in the meantime. We observe a similar behavior for $\text{Al}_{0.75}\text{Ga}_{0.25}\text{N}:\text{Si}$ with an optical threshold of $\approx 1.3 \text{ eV}$. For comparison, a PC spectrum measured at 60 K of nominally undoped AlN is also shown in Fig. 2 (dashed line). No PPC can be seen. Moreover, this undoped sample, below 50 K, shows no photoconductivity at all. Since oxygen impurities are present in similar concentrations in both samples, the absence of a photoionization threshold in nominally undoped AlN shows that the *DX*-like behavior observed in AlN:Si is indeed due to Si incorporation.

The temperature dependent conductivity of AlN:Si for an

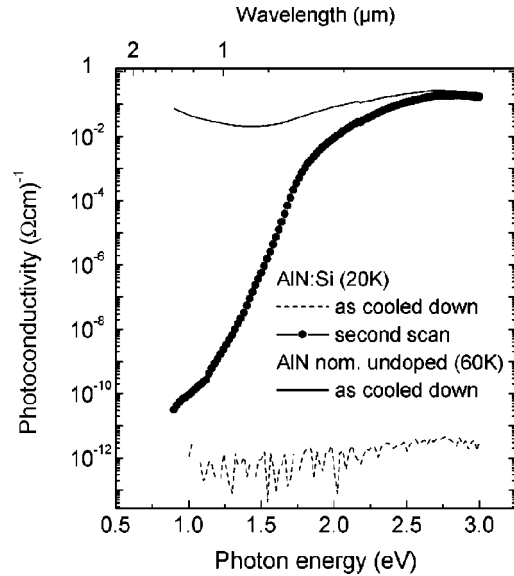


FIG. 2. Photoconductivity spectra of Si-doped AlN at 20 K. The symbols represent the spectrum recorded after cooling down the sample in the dark, the full line stands for the spectrum after illumination. The dashed line shows a PC spectrum of a nominally undoped AlN sample at 60 K. At lower temperatures, no PC can be detected.

electric field of 200 V/cm is shown in Fig. 3. Upon cooling down from room temperature to 130 K in the dark, an activated behavior with the already mentioned activation energy of 320 meV is observed (cf. Fig. 1). At 20 K, the sample has become highly resistive. Illumination with light at 550 nm increases the conductivity by many orders of magnitude. Subsequently, heating of the sample to 45 K again in the dark slightly increases the conductivity. A further increase in temperature leads to quenching of the persistent photoconductivity. From 160 K on upwards, the normal activated behavior is restored.

Further experimental evidence for the *DX* behavior of Si in AlN comes from EPR measurements. Neither at room temperature nor after cooling down to 4 K is an EPR signal detected in AlN:Si at a level of $10^{16} \text{ spins/cm}^3$ per G line-

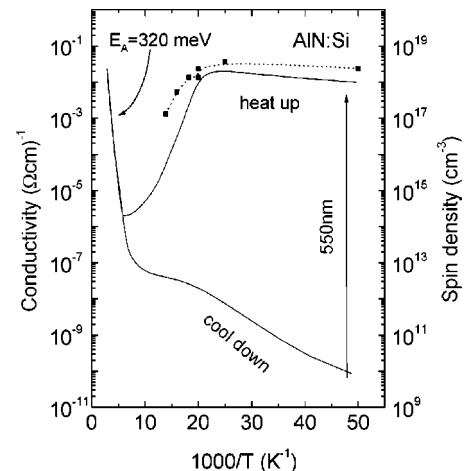


FIG. 3. Temperature dependent conductivity of AlN:Si (solid line). In addition, the spin density after illumination, as determined by EPR experiments, is also shown (full symbols).

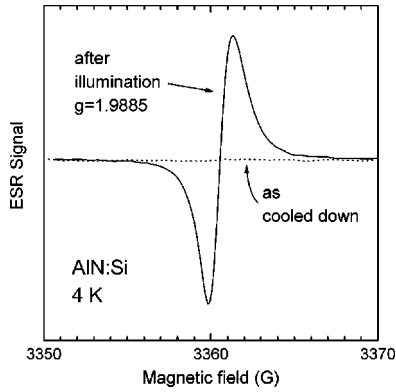
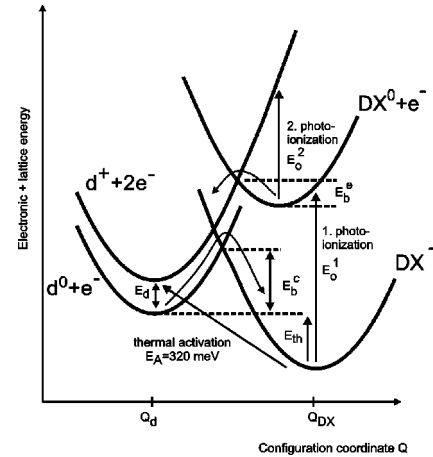


FIG. 4. EPR spectrum of AlN:Si after illumination.

width. After illumination, a strong persistent resonance with an isotropic g factor of 1.9885 ± 0.0001 appears (Fig. 4), while in GaN anisotropic donor resonances are observed.¹³ Using different edge filters to cut off the high energy end of the lamp spectrum, we confirmed that the spin density reveals the same dependence on photon energy as the photoconductivity. The signal shown in Fig. 4 was recorded at microwave powers of $16 \mu\text{W}$, since at higher powers the line shape becomes increasingly asymmetric due to electron spin to nuclear spin cross relaxation.¹⁴ The linewidth ΔH_{pp} decreases with increasing temperature, reaching a minimum of $\Delta H_{pp} = 1 \text{ G}$ at 30 K, which is consistent with the resonance being due to an impurity band rather than due to electrons in the conduction band. In an impurity band, exchange interaction leads to increased averaging of inhomogeneous hyperfine broadening with temperature, as observed for the residual donor in GaN.¹³ The dependence of the spin density on temperature after illumination at low temperature is shown in Fig. 3 (full symbols). For better comparison with the conductivity data, the same logarithmic scale is used. The spin density—as well as the conductivity—increases up to 45 K and then quickly drops below the detection limit. A maximum spin density of $3 \times 10^{18} \text{ cm}^{-3}$ is observed at 45 K. If these spins were due to mobile electrons in the conduction band, a strong free carrier absorption should be observable. However, FTIR measurements at low temperatures failed to detect such an absorption. Furthermore, assuming that the persistent photoconductivity is caused by the persistent electrons detected in EPR, we obtain a mobility of only $10^{-2} \text{ cm}^2/\text{Vs}$. Both observations, namely the missing free carrier absorption and the low mobility support the notion that the charge carriers observed in EPR are due to donor impurity band. The question whether these donor states are deep rather than shallow effective-mass-like states can be addressed by examining the observed g factor in detail. Based on a five band kp model in the quasicubic approximation, the g factors of shallow donors in GaN and $\text{Al}_x\text{Ga}_{1-x}\text{N}$ alloys with Al contents below 0.3 have been derived previously.^{13,15,16} Extending these calculations to higher Al contents and using the results of recent band structure calculations as well as experimental results for bandgap, spin-orbit splitting and electron effective mass, the experimentally observed g factor in AlN is found to be fully consistent with an effective mass donor rather than a deep state.^{17,18}

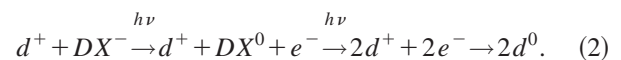
As a summary of the experimental results, we can state the following: (i) The thermal activation energy of the con-

FIG. 5. Configuration coordinate diagram of the Si DX center in AlN.

ductivity of 320 meV in n -type AlN is due to silicon incorporation. (ii) At low temperatures a photoconductivity threshold exists at about 1.5 eV photon energy. (iii) The photoconductivity persists after switching off the light. (iv) After cooling in the dark no EPR signal can be seen. (v) Upon illumination an EPR signal caused by electrons bound to a shallow effective mass state is found. (vi) The EPR signal as well as the persistent photoconductivity vanish above 60 K.

All of these results can be well explained in terms of the DX model sketched in Fig. 5. The lowest parabola represents the DX^- state, which is occupied by two electrons. This state has undergone a large lattice relaxation and is the stable ground state. The parabola above this ground state symbolizes the thermodynamically metastable DX^0 state plus one electron in the conduction band. The lower left parabola shows the substitutional—also metastable—neutral shallow donor d^0 of the Si atom, the upper left parabola represents the ionized d^+ state, both with one and two electrons in the conduction band, respectively.

Thermally, the DX^- state can emit electrons into the conduction band, which is responsible for the 320 meV activation energy and is the energy separation between the two parabola DX^- and d^+ (item i). Optical transitions, however, must be vertical in the configuration coordinate diagram and therefore the photoconductivity threshold is well above 320 meV (item ii). After photoionization of the DX^- into DX^0 , a second photoionization process $DX^0 \rightarrow d^+$ takes place. Such a two step photoionization process has already been observed by Dobaczewski and Kaczor¹⁹ for Te DX centers in $\text{Al}_x\text{Ga}_{1-x}\text{As}$, and has been shown to lead to a markedly non-exponential time dependence. At low temperatures, the d^+ state will immediately capture a free electron and thereby reform the metastable substitutional shallow donor d^0 . All together, the photoionization process can be written as



This reaction corresponds to an optical excitation out of the stable DX^- ground state into the metastable d^0 state. This state is separated from the DX^- state by an energy barrier which prevents the d^0 to undergo the DX -formation reaction

(1) and thereby return back to equilibrium. The observed persistent photoconductivity is believed to arise from hopping conduction in the defect band of the d^0 in accordance with the temperature dependence of the EPR line shape. In addition, the extremely low mobility strongly points towards transport not taking place in the conduction band. The photoconductivity is persistent because of the energy barrier E_b^c between d^0 and DX^- (item iii). From the temperature dependence of the PPC decay time constants, we can estimate the height of this barrier to (200 ± 80) meV. Although this barrier has not only an electronic part, but also an ionic one since a lattice reconstruction must take place during the $d^0 \rightarrow DX^-$ transition, we may consider this barrier—from an electronic point of view—as a capture barrier for electrons. When cooling the sample slowly in the dark, the system remains in its ground state, where DX^- and d^+ are occupied according to Eq. (1). Neither one of those two states is paramagnetic and therefore no EPR signal can be detected (item iv). In contrast, a donor with 320 meV depth would not be ionized at low temperatures and should give rise to an EPR signal. Illumination will turn the d^+ and DX^- states into two d^0 states according to Eq. (2), which cannot decay back because of the energy barrier separating the substitutional and DX configurations. The d^0 state gives rise to the observed EPR signal (item v) and the persistent photoconductivity. When the thermal energy is high enough to overcome the barrier, the equilibrium (i.e., DX^- and d^+) is restored and both, the PPC and EPR signal vanish (item vi).

Based on our experimental results, we can provide reasonable characteristic energies for the configuration diagram in Fig. 5. E_d , which would be the ionization energy of the shallow effective mass donor, can be estimated using $E_d = E_{Ry} m^* / \epsilon_{AIN}^2 = 60$ meV, where $m^* = 0.33$ has been used.¹⁷ The energy barrier between d^0 and DX^- has already been estimated to $E_b^c \approx 200$ meV. The activation energy of the conductivity at temperatures above 160 K, $E_A = 320$ meV, is given by the sum of E_d and E_{th} . Using the effective mass value for E_d results in 260 meV for E_{th} . For the optical

transition energies E_o^1 and E_o^2 , we note that the optical threshold is determined by the larger one of these two energies. Therefore an unambiguous assignment is not possible at this point.

Although this model seems to be quite consistent, some open questions remain. First, the detected spin density by EPR is about a factor of 10 below the nominal doping density. Since we have confirmed by high temperature Hall measurements (in the dark) and conductivity measurements up to 1100°C, that indeed at least 10^{19} cm⁻³ Si atoms are electrically active, we attribute this discrepancy to doping inhomogeneity of the sample. In regions with higher doping density, the Mott metal-insulator transition has taken place leading to very short spin relaxation times, which in turn broadens the resonance line width to an extent that these spins cannot be detected by EPR. Therefore, the spins observed are most likely in regions with low Si doping density. The identical photoionization threshold and temperature dependence of the PPC and EPR shows however, that the DX -like behavior is identical in low and high Si doped AlN. Furthermore we observe—especially at high electric fields—a clearly non-exponential time dependence of the photocurrent transients, which requires a more detailed discussion on the basis of rate equation modeling of the two-step photoionization.¹⁹

In conclusion, using spectrally resolved photoconductivity and EPR experiments, we have shown that Si in AlN behaves like a DX center. The observed phenomena, namely persistent photoconductivity and the lack of an equilibrium EPR signal at low temperatures, can be explained by the charge carrier driven relaxation of the shallow Si donor to the deep DX defect. The appearance of an EPR signal after illumination is well described by the metastable occupation of a shallow donor state d^0 . The energy barrier between this d^0 and the DX^- state explains the metastability as well as the quenching of the PPC and the EPR signal at temperatures above 60 K.

The authors acknowledge financial support by the Deutsche Forschungsgemeinschaft.

*Electronic mail: zeisel@wsi.tum.de

¹J. Burm, W.J. Chaff, L.F. Eastman, H. Amano, and I. Akasaki, *Appl. Phys. Lett.* **68**, 2849 (1996).

²C. Skierbiszewski, T. Suski, M. Leszczynski, M. Shin, M. Skowronski, M.D. Bremser, and R.F. Davis, *Appl. Phys. Lett.* **74**, 3833 (1999).

³D.V. Lang, in *Deep Centers in Semiconductors*, edited by S.T. Pantelides, 2nd ed. (Gordon and Breach Science Publishers, Yverdon, 1992).

⁴D.V. Lang and R.A. Logan, *Phys. Rev. Lett.* **39**, 635 (1977).

⁵D.J. Chadi, and K.J. Chang, *Phys. Rev. Lett.* **61**, 873 (1988).

⁶C.H. Park and D.J. Chadi, *Phys. Rev. B* **55**, 12995 (1997).

⁷P. Boguslawski and J. Bernholc, *Phys. Rev. B* **56**, 9496 (1997).

⁸C.G. Van de Walle, *Phys. Rev. B* **57**, R2033 (1998).

⁹C. Wetzel, T. Suski, J.W. Ager III, E.R. Weber, E.E. Haller, S. Fischer, B.K. Meyer, R.J. Molnar, and P. Perlin, *Phys. Rev. Lett.* **78**, 3923 (1997).

¹⁰M.D. McCluskey, N.M. Johnson, C.G. Van de Walle, D.P. Bour, M. Kneissl, and W. Walukiewicz, *Phys. Rev. Lett.* **80**, 4008 (1998).

¹¹M.T. Hirsch, J.A. Wolk, W. Walukiewicz, and E.E. Haller, *Appl. Phys. Lett.* **71**, 1098 (1997).

¹²J.Z. Li, J.Y. Lin, H.X. Jiang, M. Asif Khan, and Q. Chen, *J. Appl. Phys.* **82**, 1227 (1997).

¹³W.E. Carlos, J.A. Freitas, M. Asif Khan, D.T. Olson, and J.N. Kuznia, *Phys. Rev. B* **48**, 17878 (1993).

¹⁴G. Denninger, R. Beerhalter, D. Reiser, K. Maier, J. Schneider, T. Detchprohm, and K. Hiramoto, *Solid State Commun.* **99**, 347 (1996).

¹⁵W. E. Carlos, in *Seventh International Conference on Shallow-Level Centers in Semiconductors*, edited by C. A. J. Ammerlaan and B. Pajot (World Scientific, Singapore, 1997), p. 13.

¹⁶D.J. Chadi, A.H. Clark, and R.D. Burnham, *Phys. Rev. B* **13**, 4466 (1976).

¹⁷J.A. Majewski, M. Städele, and P. Vogl, *Mater. Res. Soc. Symp. Proc.* **449**, 887 (1997).

¹⁸W. Knap *et al.*, *Appl. Phys. Lett.* **70**, 2123 (1997).

¹⁹L. Dobaczewski and P. Kaczor, *Phys. Rev. Lett.* **66**, 68 (1991).